

# Turbulence closure in the light of phase transition

Mohammed A. Azim

Department of Mechanical Engineering, Bangladesh University of Engineering and Technology, Dhaka-1000, Bangladesh, email: azim@me.buet.ac.bd

In the present study, new turbulence closure equations are derived in the light of continuous (often termed second order) phase transition. Closed form Reynolds averaged Navier-Stokes equations due to those closure equations are solved numerically for a plane turbulent free jet. There turbulent viscosity is treated as a tensor unlike the eddy viscosity. An overall agreement of the obtained results with the existing literature for the jet flow proves the effectiveness of the new closure equations. Besides, turbulent stresses as a function of normalized mean velocity are found to exhibit their odd and even symmetries which seem to be the manifestations of the free energy symmetry of continuous phase transition.

**Keywords:** phase transition, free energy, order parameter, symmetry, closure equation, viscosity tensor.

## 1. Introduction

Turbulent flow is characterized by a hierarchy of scales of fluctuations ranging from production to dissipation. The dynamics of turbulent flow is governed by the Navier-Stokes equations whose solution resolving all those scales at high Reynolds number in complex geometries is unlikely to be attainable in the foreseeable future. However, Reynolds averaging and filtering are the two methods that have been used to transform the Navier-Stokes equations in such a way that the small-scale turbulent fluctuations do not have to be directly simulated. Both methods introduce additional terms in the governing equations due to the correlations of fluctuating quantities (i.e. turbulent stresses) that need to be modeled in order to achieve closure. The closure assures a sufficient number of equations for all the unknowns. Turbulence modeling requires that turbulent stresses in the Reynolds averaged Navier-Stokes (RANS) equations be appropriately modeled<sup>1</sup>. Boussinesq hypothesis<sup>2</sup> is the core of all turbulence models that relates the Reynolds stresses to the mean velocity gradients as

$$-\overline{u'_i u'_j} = \nu_T \left( \partial \overline{u}_i / \partial x_j + \partial \overline{u}_j / \partial x_i \right) \quad (1)$$

for incompressible fluid which is analogous to the laminar one with enlarged viscosity called the eddy viscosity. This eddy viscosity requires further modeling as, for example,  $\nu_T = \ell_m^2 (\partial \overline{u} / \partial y)$  after Prandtl<sup>3</sup>,  $\nu_T = C_\mu \ell_m \sqrt{k}$  after Kolmogorov<sup>4</sup> and Prandtl<sup>5</sup>,  $\nu_T = C_\mu k^2 / \varepsilon$  after Launder and Spalding<sup>6</sup>, where  $\ell_m$  is the mixing length (closely related to the length scale).

Present endeavor aims at extracting turbulence closure equations by using the features of continuous (also called second order) phase transition against the order parameter. The concept of order parameter in

phase transition has been widely generalized as when an arbitrary system crosses an instability point, only just a few variables become relevant and serves as order parameter which may be a single or coupled variables that distinguishes the ordered from the disordered phase. However, the averaged velocity may be a suitable control parameter for a fluid dynamical system which if adequately tuned, the system can undergo strong qualitative changes in its macroscopic properties and consequently in microscopic properties. Goldenfeld<sup>7</sup> showed that the rise of temperature in metals is similar to the increase in velocity in the fluid flows, the former causes magnetization at critical point and the latter turbulence. This invokes strong analogy between the turbulization and the magnetization at critical point<sup>7-9</sup>. Recently many researchers have demonstrated both experimentally and numerically by resolving the time and length scales sufficiently close to the critical point that all turbulent flows are closely analogous to the continuous phase transition<sup>10-13</sup>. In continuous phase transition, Landau free energy<sup>14</sup> of a system exhibits symmetry against the order parameter. This free energy of the system and the kinetic energy of turbulence are analogous because both near their critical points obey the power-law scaling of the correlation functions<sup>15</sup>.

## 2. Closure equations due to phase transition

Navier-Stokes equations represent the collective motion of fluid particles. These equations of motion for incompressible fluid are

$$\frac{\partial \overline{u}_i}{\partial t} + \overline{u}_j \frac{\partial \overline{u}_i}{\partial x_j} = - \frac{\partial}{\partial x_j} \left( \frac{\overline{p}}{\rho} \delta_{ij} + \overline{u'_i u'_j} \right) + \nu \frac{\partial^2 \overline{u}_i}{\partial x_j^2} \quad (2)$$

In collective motion, the most naturally (but not necessarily) chosen order parameter is the averaged velocity<sup>16</sup>. The concept of moving equilibrium<sup>17</sup> states

that the rate of change of each component of Reynolds stress  $\overline{u'_i u'_j}$  is proportional to the rate of change of turbulence kinetic energy  $k$ , that is,  $\overline{u'_i u'_j}$  corresponds to the free energy of phase transition.

In view of relating the features of phase transition to the dynamics of turbulence, an implicit function  $f(\overline{u}_i, t) = 0$  for RANS equation (2) is written as

$$f(\overline{u}_i, t) = \frac{\partial \overline{u}_i}{\partial t} + \overline{u}_j \frac{\partial \overline{u}_i}{\partial x_j} + \frac{\partial}{\partial x_j} \left( \frac{\overline{p}}{\rho} \delta_{ij} + \overline{u'_i u'_j} \right) - \nu \frac{\partial^2 \overline{u}_i}{\partial x_j^2} \quad (3)$$

where  $\overline{p}$  and  $\overline{u'_i u'_j}$  are functions of  $\overline{u}_i$ . The differential form of the implicit function is  $(\partial f / \partial \overline{u}_i) d\overline{u}_i + (\partial f / \partial t) dt = 0$  which on holding the time constant yields  $\partial f / \partial \overline{u}_i = 0$  because  $d\overline{u}_i(x_j) = 0$  is unrealistic. The equation  $\partial f / \partial \overline{u}_i = 0$  is the first derivative of the free energy (RANS equation) against the order parameter  $\overline{u}_i$  holding the time constant that expresses the state of turbulence in terms of free energy equilibrium. Hence, this equation combines the two phenomena, turbulence and phase transition, leading to

$$\frac{\partial}{\partial \overline{u}_i} \frac{\partial}{\partial x_j} \left( \frac{\overline{p}}{\rho} \delta_{ij} + \overline{u'_i u'_j} \right) = 0 \quad (4)$$

for being  $\partial(\overline{u}_j \partial \overline{u}_i / \partial x_j) / \partial \overline{u}_i = \partial(d\overline{u}_i / dt - \partial \overline{u}_i / \partial t) / \partial \overline{u}_i$  that equals zero. Equation (4) can be written by using the chain rule for  $\overline{u}_j = \overline{u}_j(x_j)$  and using an entity  $f_1(\overline{u}_i) \delta_{kj} \partial \overline{u}_k / \partial x_j = 0$  due to the continuity equation as

$$\frac{\partial}{\partial \overline{u}_i} \frac{\partial}{\partial \overline{u}_k} \left( \frac{\overline{p}}{\rho} \delta_{ij} + \overline{u'_i u'_j} \right) \frac{\partial \overline{u}_k}{\partial x_j} = f_1(\overline{u}_i) \delta_{kj} \frac{\partial \overline{u}_k}{\partial x_j} \quad (5)$$

where the function  $f_1(\overline{u}_i)$  is ascertained later. This equation through manipulation may be written for each component of  $\overline{u'_i u'_j}$  as

$$\frac{\partial}{\partial \overline{u}_i} \frac{\partial}{\partial \overline{u}_k} \left( \frac{\overline{p}}{\rho} \delta_{ij} + \overline{u'_i u'_j} \right) = f_1(\overline{u}_i) \delta_{kj} \quad (6)$$

which upon integration yields

$$\overline{u'_i u'_j} = -\frac{\overline{p}}{\rho} \delta_{ij} + \iint f_1(\overline{u}_i) \delta_{kj} d\overline{u}_i d\overline{u}_k \quad (7)$$

and on replacing the index  $k$  by  $j$  becomes

$$\overline{u'_i u'_j} = C_{(i)(j)} \left( -\frac{\overline{p}}{\rho} \delta_{ij} + \iint f_1(\overline{u}_i) d\overline{u}_i d\overline{u}_j \right) \quad (8)$$

where  $C_{ij}$  are the scaling constants for a balance between the turbulent and the mean quantities of the equation. The indices  $(i)$  and  $(j)$  in the parentheses indicate that they are not summed over. By interchanging the position of indices  $i$  and  $j$ , for off-diagonal symmetry of  $\overline{u'_i u'_j}$ , turbulence closure equation (8) becomes in the final form as

$$\overline{u'_i u'_j} = C_{(i)(j)} \left( -\overline{p} \delta_{ij} / \rho + \frac{1}{2} \iint \{ f_1(\overline{u}_i) + f_1(\overline{u}_j) \} d\overline{u}_i d\overline{u}_j \right) \quad (9)$$

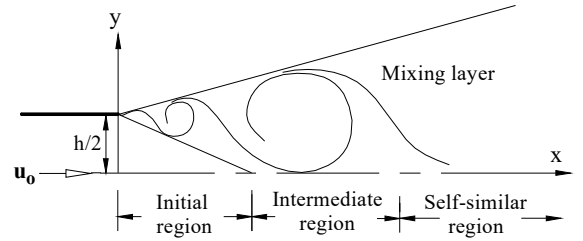


Fig. 1 Schematic of a plane turbulent jet.

### 3. Application to a plane jet flow

The derived closure equations are applied to unclosed RANS equations for a plane jet as a test case. Plane jets are free shear flows where fluids coming out from two-dimensional (2D) orifice mix with the ambient fluid and develop through three successive distinct regions, namely initial, intermediate and developed regions (Fig. 1). Initial region (at  $x/h \leq 6$ ) is characterized by the presence of a potential core of uniform axial velocity that is in laminar state, intermediate region by the transition state and developed region by the turbulent state. Literature<sup>18</sup> shows a large scatter of the downstream distance at which the jet becomes fully developed, ranging from  $5h$  to  $25h$ , depending on its initial conditions (e.g. Reynolds number at exit and nozzle geometry). This jet grows non-linearly in the developing (initial and intermediate) region and linearly in the developed (self-similar) region. The governing equations and their initial and boundary conditions, and determination of the constants  $C_{ij}$  and function  $f_1(\overline{u}_i)$ , the closure equations in  $(x, y, z)$  coordinates and the description on Reynolds stress plotting are presented in this section.

### 3.1 Governing equations

Continuity and RANS equations describing a steady plane turbulent jet flow for incompressible fluid are

$$\frac{\partial \bar{u}_i}{\partial x_i} = 0 \quad (10)$$

$$\bar{u}_j \frac{\partial \bar{u}_i}{\partial x_j} = -\frac{1}{\rho} \frac{\partial \bar{p}}{\partial x_i} + \frac{\partial}{\partial x_j} \left( \nu \frac{\partial \bar{u}_i}{\partial x_j} - \overline{u'_i u'_j} \right) \quad (11)$$

where  $-\overline{u'_i u'_j} = \nu_{T(i)(j)} (\partial \bar{u}_i / \partial x_j + \partial \bar{u}_j / \partial x_i)$  is the turbulent stress-strain rate relation and  $\nu_{Tij}$  the turbulent viscosity tensor. Equations (9)-(11) are in closed form and need to be solved for extracting mean and turbulence quantities of the flow.

### 3.2 Initial and boundary conditions

In free jet flow, the initial conditions are  $\bar{u}(0, y \leq 0.5h) = u_o$ ,  $\bar{u}(0, y > 0.5h) = 0$  and  $\bar{v}(0, y) = 0$  where  $h$  is the orifice height and  $u_o$  the uniform jet exit velocity. The boundary conditions are  $\phi$  (general flow variable) attains ambient conditions at the jet outer edge,  $\partial \phi / \partial x = 0$  at the outflow, and  $\partial \phi / \partial y = 0$  at the symmetry axis except  $\bar{v} = 0$  and  $\overline{u'v'} = 0$ .

### 3.3 Determination of $C_{ij}$

The concept of moving equilibrium<sup>17</sup> may be read in explicit form as

$$\overline{u'_i u'_j} = a_{(i)(j)} (\delta_{ij} \pm \varepsilon_{ijk}) k \quad (12)$$

where  $a_{ij}$  are the proportionality constants. From Eqs. (9) and (12), it can be written that

$$\overline{u'_i u'_j} \sim \left( -\frac{\bar{p}}{\rho} \delta_{ij} + \frac{1}{2} \iint \{ f_1(\bar{u}_i) + f_1(\bar{u}_j) \} d\bar{u}_i d\bar{u}_j \right) \sim (\delta_{ij} \pm \varepsilon_{ijk}) k. \quad (13)$$

This equation indicates that  $C_{ij}$  of Eq. (9) and  $a_{ij}$  of Eq. (12) are structurally similar, and hence  $a_{ij} = C_o C_{ij}$  for  $C_o$  is a constant. Now using the relations  $\overline{u'v'} / \sqrt{\overline{u'u'}} \sqrt{\overline{v'v'}} \approx 0.46$  and  $\overline{u'v'} / k \approx 0.35$  for the turbulent flows and  $\overline{u'u'} \approx 1.3 \overline{v'v'}$  for plane jet flow<sup>19</sup> along with Eq. (12), the constants are evaluated to be  $a_{11} = 0.87$ ,  $a_{22} = 0.67$  and  $a_{12} = 0.35$ . The values of  $C_{ij}$  are calculated later by knowing the value of  $C_o$ .

### 3.4 $f_1(\bar{u}_i)$ and closure equations in $(x, y, z)$

The free energy of turbulence  $\overline{u'_i u'_j}$  may be expressed by a fourth degree polynomial of normalized

velocity  $\bar{u}/u_c$  ( $u_c$  is the jet centerline velocity) with a view to capture the free energy symmetry of continuous phase transition. Here  $\bar{u}$ -velocity is the only order parameter because  $\bar{v}$ -velocity does not vary enough smoothly over the co-ordinates like the turbulent stresses. Analysis of turbulent shear stress data of plane and circular jets<sup>20-21</sup> show that the coefficient of the fourth order term is insignificant compared to other coefficients of that polynomial in the initial region of the jet while the same is larger than or comparable to other coefficients in the intermediate and self-similar regions. Furthermore, the coefficients of the second order term of the polynomials higher than the fourth degree are found small, which is not consistent with the order of magnitude estimate of  $\overline{u'v'}$  by dimensional analysis. It seems now that  $\overline{u'v'}$  is best expressed by a third degree polynomial of  $\bar{u}/u_c$  in the initial region of the jet and by a fourth degree polynomial beyond the initial region. Such a polynomial may be assumed as  $-\overline{u'v'}/u_c^2 = C_s (U - U^2 + U^3 - U^4)$  for the shear stress. Turbulent shear stresses in general are symmetric with respect to the origin (called odd symmetric) while the normal stresses are symmetric with respect to the axis (called even symmetric). Hence, turbulent normal stress function may be obtained by integrating the above polynomial as

$$\overline{u'u'}/u_c^2 = C_n U \left( 1 - \frac{1}{2}U + \frac{1}{3}U^2 - \frac{1}{4}U^3 + \frac{1}{5}U^4 + \text{rest} \right),$$

which further can be approximated as  $\overline{u'u'}/u_c^2 = C_n U \exp(-\alpha U)$  where  $U = \bar{u}/u_c$ , and  $C_s$ ,  $C_n$  and  $\alpha$  are constants. This is because an odd symmetric function either by differentiation once or by integration becomes even symmetric and vice-versa. Similar to Landau free energy expansion<sup>14</sup>, a term may be added to the turbulent normal stress function as  $\overline{u'u'}/u_c^2 = C_n U \exp(-\alpha U) + C_d (0.5U^2U)$  where  $C_d$  is a constant and  $0.5U^2U$  corresponds to the entropic energy, resulting from the coupling of mean motion energy and order parameter, which is transferred to the surrounding as dissipated heat. Here, the order parameter may be defined in order that the coefficient  $C_d$  reduces to unity.

The function  $f_1(\bar{u})$  for the Reynolds stresses are obtained from Eq. (7), discarding the pressure term, by using their functional form for the normal stress and by using the highest order term of the polynomial for the shear stress. The derived function  $f_1(\bar{u})$  for the axial normal stress  $\overline{u'u'}$  is  $f_u(\bar{u}) = \partial^2 (\overline{u'u'}) / \partial u \partial u$ , i.e.

$$f_u(\bar{u}) = C_n u_c \beta (-2 + \beta \bar{u}) \exp(-\beta \bar{u}) + 3C_d \bar{u}/u_c \quad (14a)$$

where  $\beta = a/u_c$ , for the transverse normal stress  $\overline{v'v'}$  is  $f_v(\bar{u}) = \partial^2(\overline{v'v'})/\partial v \partial v$ , i.e.

$$f_v(\bar{u}) = (a_{22}/a_{11}) \left( \frac{\partial \bar{u}}{\partial v} \right)^2 f_u(\bar{u}) \quad (14b)$$

and for the shear stress  $\overline{u'v'}$  is

$$f_s(\bar{u}) = (a_{11}/a_{12}) \partial^2(\overline{u'v'})/\partial u \partial u. \quad (14c)$$

That is  $f_s(\bar{u}) = C_s \bar{u}/u_c$  for the initial region of the jet and  $f_s(\bar{u}) = C_s \bar{u}^2/u_c^2$  beyond the initial region. The highest order term is used instead of entire polynomial for the shear stress as this requires known values of the coefficients that might cause ascertaining  $f_s(\bar{u})$  unlikely. Further, the function  $f_s(\bar{u})$  is the second derivative of the highest order term of the polynomial, as a result, retains the same characteristics of  $f_s(\bar{u})$  if were obtained by using the entire polynomial. The above reasons justify the use of the highest order term instead of the entire polynomial in determining  $f_s(\bar{u})$  for the turbulent shear stress.

Using the functions  $f_u(\bar{u})$ ,  $f_v(\bar{u})$  and  $f_s(\bar{u})$ , closure equation (8) upon integration become in  $(x,y,z)$  coordinates as

$$\overline{u'u'} = C_{11} \left( -\frac{\bar{p}}{\rho} + \iint f_u(\bar{u}) d\bar{u} d\bar{u} \right) \quad (15a)$$

$$\overline{v'v'} = C_{22} \left( -\frac{\bar{p}}{\rho} + \frac{C_{22}}{C_{11}} \iint f_u(\bar{u}) d\bar{u} d\bar{u} \right) \quad (15b)$$

$$\overline{u'v'} = C_{12} \iint f_s(\bar{u}) d\bar{u} d\bar{v}. \quad (15c)$$

### 3.5 Plotting of Reynolds stresses

Equation (15a) may be written by using  $\bar{u} = \bar{u}(y)$  across the stream as

$$\overline{u'u'} = C_{11} \left( -\frac{\bar{p}}{\rho} + \iint f_u(\bar{u}) \left( \frac{\partial \bar{u}}{\partial y} \right)^2 dy dy \right) \quad (16)$$

where  $\bar{u}(y)$  is an even function. Let the normal stresses given by Eq. (15a) and Eq. (16) are denoted by  $\overline{u'u'}$  and  $\overline{u'u'}^y$  while their plots against  $y$ -axis are not equal in area because of the difference in integration intervals across the stream that lies between the outer edge and centerline of the jet for the former equation, and between the two outer edges for the latter equation.

Hence,  $\int \overline{u'u'}^y dy' = \int \overline{u'u'} dy$  where  $y'$  and  $y$  are assumed to be related by  $y' = \lambda y$  for  $\lambda$  is a constant.

The constant can be calculated as  $\lambda = \int \overline{u'u'}^y dy' / \int \overline{u'u'} dy$  and the Reynolds stresses must be plotted against  $y' = \lambda y$ .

## 4. Numerical strategies

A CFD (Computational Fluid Dynamics) code is developed for solving 2D steady flow based on finite volume method and rectangular structured grid<sup>22</sup>. SIMPLE (Semi-Implicit Method for Pressure Linked Equations) algorithm of Patankar and Spalding<sup>23</sup> is employed to solve the equations (9)-(11) governing the plane turbulent free jet. Discretization of the governing equations, computational grids and grid convergence test are described in this section.

### 4.1 Discretization and computational grids

The convective and diffusive terms of the transport equations for  $\phi$  are discretized using the second-order upwind difference scheme and the second-order central difference scheme in staggered grid, respectively, with cell centers for  $\bar{u}$  at  $(i,J)$ , for  $\bar{v}$  at  $(I,j)$ , for  $\bar{p}$ ,  $\overline{u'u'}$  and  $\overline{v'v'}$  at  $(I,J)$ , and for  $\overline{u'v'}$  at  $(i,j)$ . The discretized equations are solved iteratively using the line by line tridiagonal matrix algorithm<sup>24</sup> (TDMA). The momentum and pressure correction equations are provided with suitable number of sweeps. All variables  $(\bar{u}, \bar{v}, \bar{p})$  are weighted with very low under-relaxation factors (order of 0.1) for stability of the numerical scheme. The flow variables are expressed further by a weighted average of their neighbors in each iteration after obtaining them by using TDMA. This procedure ensures stability of the numerical scheme by reducing the oscillations of strain rates in turbulent viscosity calculation from the stress-strain rate relation.

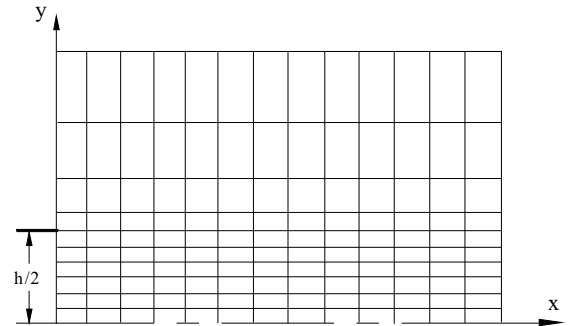


Fig. 2 Computational grids for a plane turbulent jet.

The flow domain is constructed over  $40h \times 20h$  in  $x$  and  $y$ -directions with grids as in Fig. 2. Grids are

uniform inside the orifice and varying outside it in  $y$ -direction, and uniform in  $x$ -direction as in the figure. The solutions are considered converged if the mean flow features become established and the normalized residuals become nearly constant. The attained nearly constant mass residual is  $6.8 \times 10^{-5}$  while other residuals are lower than this value. Figure 3 presents the convergence history of the numerical scheme by a residual plot against the number of iterations.

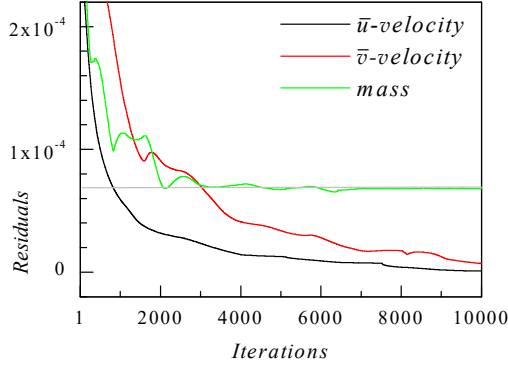


Fig. 3 Convergence of the numerical scheme.

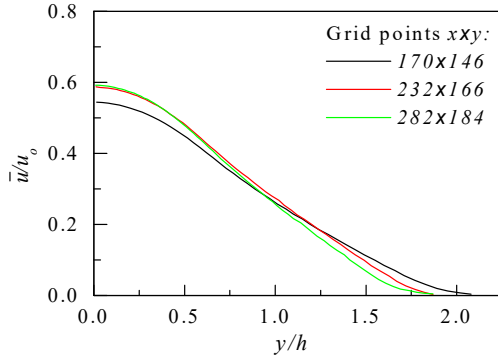


Fig. 4 Axial mean velocity profiles at  $x/h=5$ .

#### 4.2 Grid convergence test

Present simulation is performed for a plane turbulent free jet with Reynolds number  $Re=3.2 \times 10^4$ , orifice height  $h=0.04m$  and velocity at exit  $u_o=12 m/s$ . A grid convergence test is carried out with the three grid sizes termed coarse, medium and fine which are  $170 \times 146$ ,  $232 \times 166$  and  $282 \times 184$  in  $x \times y$ - directions having a grid refinement factor of 1.45 between the coarse and fine grids. Figure 4 depicts the transverse profiles of mean axial velocity at  $x/h=5$  for the three grid sets. Grid refinement shows successful convergence for those three grid resolutions. The results presented here are obtained by using the fine mesh.

## 5. Results and discussion

Closed form RANS equations (9)-(11), governing the turbulent flow, are solved numerically for a plane jet. The used numerical scheme is found to produce stable solution for  $C_{11}=0.048$ ,  $C_{22}=0.037$  and  $C_{12}=0.019$  that are obtained by using the relation  $C_{ij} = a_{ij}/C_o$  for a minimum value of  $C_o \approx 18.2$ . Values of other constants appearing in the functions  $f_1(\bar{u})$  for turbulent shear and normal stresses within the stable numerical scheme are found to be  $C_s=382.2$ ,  $C_n=3.1$  and  $C_d=1.64$  for the entire jet flow while  $\alpha=3$  for the initial region and  $\alpha=2$  beyond the initial region. Two values of  $\alpha$  provide two expressions for  $f_u(\bar{u})$  similar to that for  $f_s(\bar{u})$ . This section presents axial velocity, transverse velocity, and turbulent stresses that are extracted from the present simulation, and their comparison with the existing theoretical<sup>18</sup>, experimental (Exp) and numerical data on planar turbulent jets. Klein *et al.*<sup>19</sup> performed direct numerical simulation (DNS) of a turbulent plane jet with  $Re=4 \times 10^3$  and compared their results (e.g. mean velocity and Reynolds stresses) with the results of several authors and found in good agreement. Heschl *et al.*<sup>20</sup> made RANS simulation of plane jet with  $Re=3 \times 10^4$  using the standard  $k-\epsilon$  turbulence model and compared their results with the existing experimental data. Ramaprian and Chandrasekhara<sup>25</sup> with  $Re=1.6 \times 10^3$  have investigated experimentally the plane jets and presented the profiles of mean velocity and turbulent stresses.

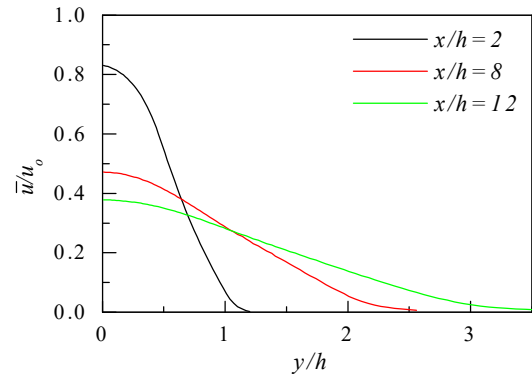


Fig. 5 Axial mean velocity profiles.

Mean axial velocity  $\bar{u}/u_o$  is presented in Fig. 5 against the transverse distance  $y/h$  at axial locations  $x/h=2, 8$  and  $12$ . This figure illustrates that the jet grows with the axial distance due to the entrainment of ambient fluid and its maximum velocity decreases due

to the loss of momentum by the interaction with the ambient fluid. Figure 6 presents normalized mean velocity  $\bar{u}/u_c$  against  $y/y_{1/2}$  at axial location  $x/h=12$  along with Gaussian curve<sup>18</sup> of the form  $\bar{u}/u_c = \exp(-0.693\eta^2)$  and DNS results<sup>19</sup> where  $\eta=y/y_{1/2}$  and  $y_{1/2}$  is the jet's half-width. The figure shows that results from the present simulation and DNS compare well with the Gaussian curve. Transverse velocity  $\bar{v}/u_c$  is depicted in Fig. 7 against  $y/y_{1/2}$  at axial locations  $x/h=8$  and 12. The figure shows that  $\bar{v}$ -velocity profiles have achieved free-stream value. DNS<sup>19</sup> and experimental<sup>25</sup> data for  $\bar{v}$ -velocity provided in the figure are in satisfactory agreement with the present simulation.

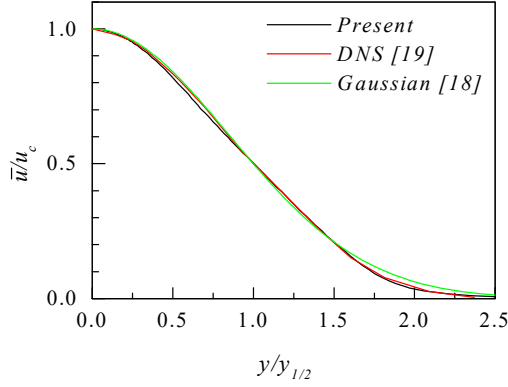


Fig. 6 Normalized axial mean velocity at  $x/h=12$ .

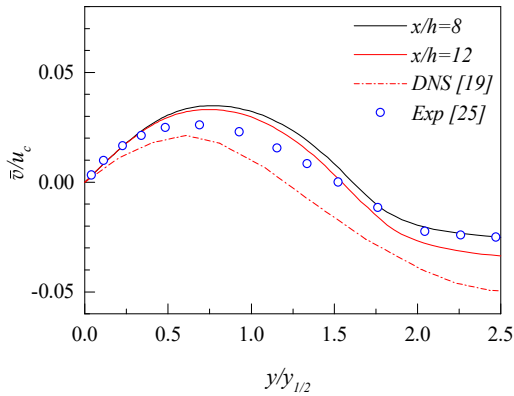


Fig. 7 Transverse mean velocity profiles.

Reynolds normal stresses  $\overline{u'u'}/u_c^2$  and  $\overline{v'v'}/u_c^2$ , and shear stress  $\overline{u'v'}/u_c^2$  are calculated in this simulation

from Eq. (15) and plotted in Figs. 8-10 against  $y/y_{1/2}$  at  $x/h=8$  and 12 for  $\lambda \approx 1.43$  (a constant appeared in Sec. 3.5). Calculated stresses from DNS<sup>19</sup>, RANS simulation<sup>20</sup> and measurement<sup>25</sup> are added for comparison in those figures. All turbulent stresses from the present simulation,  $\overline{u'u'}$  in Fig. 8,  $\overline{v'v'}$  in Fig. 9 and  $\overline{u'v'}$  in Fig. 10, are observed in close agreement with the stresses from measurement and simulations.

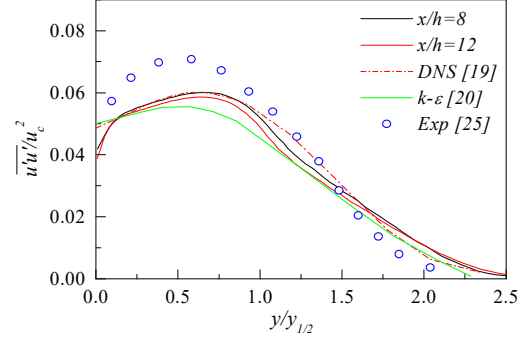


Fig. 8. Axial normal stress profiles.

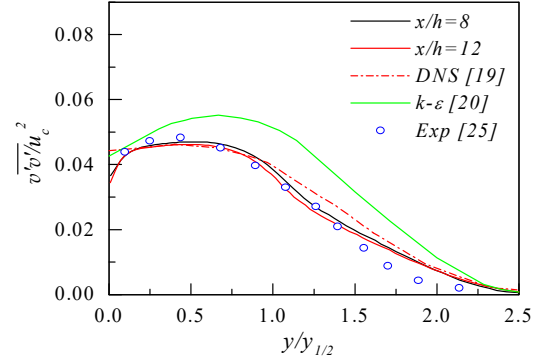


Fig. 9 Transverse normal stress profiles.

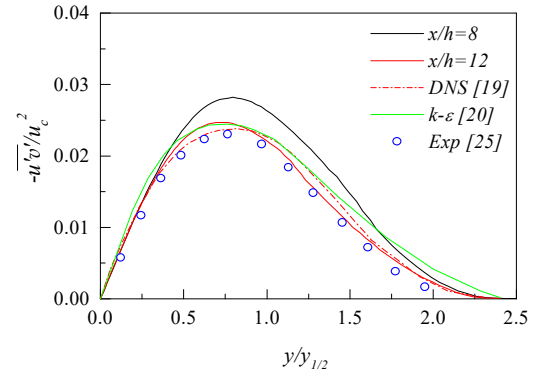


Fig. 10 Reynolds shear stress profiles.

## 6. Conclusions

The new closure equations derived by considering turbulence as continuous phase transition are utilized here to get the closed form RANS equations. Numerical solution of those equations for a plane jet flow provides the mean axial and transverse velocities, and turbulent stresses. Extracted results from the simulation are found in overall agreement with the existing data that shows the effectiveness of the closure equations. Turbulent stresses of the jet as a function of normalized mean velocity confirm their odd and even symmetries, and owing of additional terms like the one in Landau free energy expansion<sup>14</sup> and thus demonstrate the phenomenological relations with phase transition and restate that laminar-turbulent transition undergoes a continuous phase transition.

## References

- <sup>1</sup>O. Reynolds, On the dynamical theory of incompressible viscous fluids and determination of the criterion, *Phil. Trans. Roy. Soc. A* 186, 123 (1895).
- <sup>2</sup>J. Boussinesq, *Theorie de l'ecoulement tourbillant*, *Mem. Pres. Acad. Sci.* 23, 46 (1877).
- <sup>3</sup>L. Prandtl, Über die ausgebildete turbulenz, *ZAMM* 5, 136 (1925).
- <sup>4</sup>A.N. Kolmogorov, Equations of turbulent motion of an incompressible fluid, *Izv. Acad. Nauk USSR, Ser. Fiz.* 6, 56 (1942).
- <sup>5</sup>L. Prandtl, Über ein neues formelsystem für die ausgebildete turbulenz, *Nachr. Akad. Wiss. Göttingen, Math.-Phys.Kl.*, 6 (1945).
- <sup>6</sup>B.E. Launder and D.B. Spalding, *Mathematical Models of Turbulence* (Academic Press, London, 1972).
- <sup>7</sup>N. Goldenfeld, Roughness induced critical phenomena in a turbulent flow, *Phys. Rev. Lett.* 96, 044503 (2006).
- <sup>8</sup>S.T. Bramwell, P.C. W. Holdsworth, and J.-F. Pinton, Universality of rare fluctuations in turbulence and critical phenomena, *Nature* 396, 552 (1998).
- <sup>9</sup>Ch. Chatelain, P.E. Berche and B. Berche, Second-order phase transition induced by deterministic fluctuations in aperiodic eight-state Potts models, *Eur. Phys. J. B* 7, 439 (1999).
- <sup>10</sup>W.S. Gan, Application of spontaneous broken symmetry to turbulence, *Proc. ICSV16, Krakow, Poland* (2009).
- <sup>11</sup>K. Avila, D. Moxey, A. de Lozar, M. Avila, D. Barkley and B. Hof, The onset of turbulence in pipe flow, *Science* 333, 192 (2011).
- <sup>12</sup>N. Vladimirova, S. Derevyanko, and G. Falkovich, Phase transitions in wave turbulence, *Phys. Rev. E* 85, 010101 (2012).
- <sup>13</sup>L. Shi, G. Lemoult, K. Avila, S. Jalikop, M. Avila and B. Hof, The universality class of the transition to turbulence, *arXiv:1504.03304, physics.flu-dyn* (2015).
- <sup>14</sup>P. C. Hohenberg and A. P. Krekhov, An introduction to the Ginzburg-Landau theory of phase transitions and nonequilibrium patterns, *arXiv:1410.7285, cond-mat* (2015).
- <sup>15</sup>N. Goldenfeld and H.-Y. Shih, Turbulence as a problem in non-equilibrium statistical mechanics, *J. Stat. Phys.* 167, 575 (2017).
- <sup>16</sup>T. Vicsek and A. Zafeiris, Collective motion, *Phys. Reports* 517, 71 (2012).
- <sup>17</sup>P.A. Durbin and B.A.P. Reif, *Statistical Theory and Modeling for Turbulent Flows* (John Wiley and Sons, 2011).
- <sup>18</sup>R.C. Deo, J. Mi and G.J. Nathan, The influence of Reynolds number on a plane jet, *Phys. Fluids* 20, 075108 (2008).
- <sup>19</sup>M. Klein, A. Sadiki and J. Janicka, Investigation of the influence of the Reynolds number on a plane jet using direct numerical simulation, *Int. J. Heat and Fluid Flow* 24, 785 (2003).
- <sup>20</sup>C. Heschl, K. Inthavong, W. Sanz and J. Tu, Evaluation and improvements of RANS turbulence models for linear diffuser flows, *Computers & Fluids* 71, 272 (2013).
- <sup>21</sup>H. Fellouah, C.G. Ball and A. Pollard, Reynolds number effects within the development region of a turbulent round free jet, *Int. J. Heat and Mass Transfer* 52, 3943 (2009).
- <sup>22</sup>M.A. Azim, Numerical study of closely spaced twin circular jets, *Int. J. Fluid Mech. Res.* 47, 407 (2020).
- <sup>23</sup>S.V. Patankar and D.B. Spalding, A calculation procedure for heat, mass and momentum transfer in three dimensional parabolic flows, *Int. J. Heat Mass Transfer* 15, 1787 (1972).
- <sup>24</sup>L.H. Thomas, Elliptic problems in linear difference equations over a network, *Watson Sci. Comput. Lab. Report, Columbia University, New York* (1949).
- <sup>25</sup>B.R. Ramaprian and M.S. Chandrasekhara, LDA measurements in plane turbulent jets, *ASME J. Fluids Eng.* 107, 264 (1985).